HNPS Advances in Nuclear Physics

Vol 7 (1996)

HNPS1996

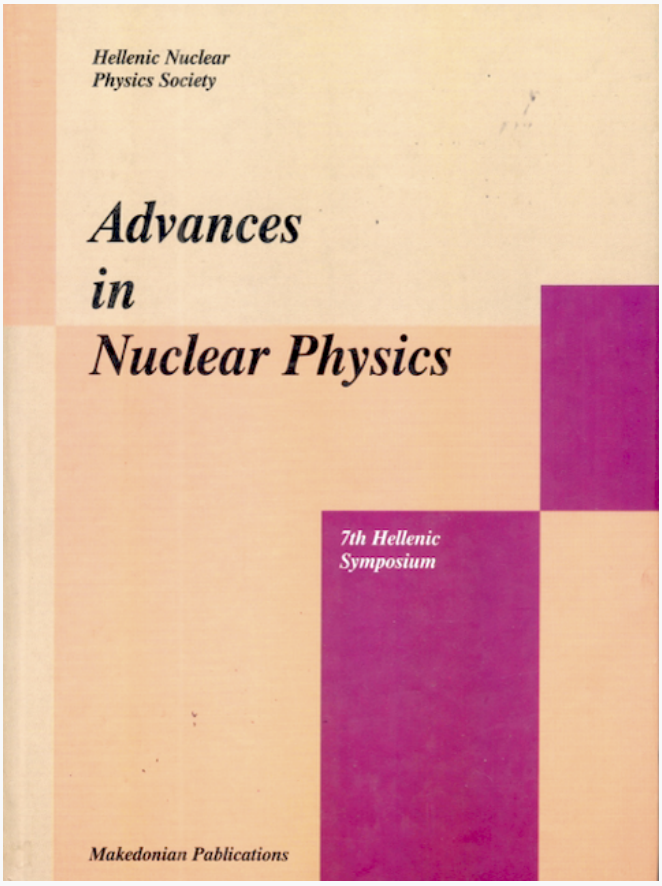

Decay of 160Er* in 16O + 144Nd and 64Ni + 96Zr Fusion Reactions

N. G. Nicolis, J. L. Barreto, D. G. Sarantites, R. J. Charity, L. G. Sobotka, D. W. Stracener, D. C. Hensley, J. R. Beene, C. Baktash, M. L. Halbert, M. Thoennessen

doi: 10.12681/hnps.2410

Decay of $^{160}Er^*$ in $^{16}O + ^{144}Nd$ and $^{64}Ni + ^{96}Zr$ Fusion Reactions

N.G. Nicolis [a], J.L. Barreto [a], D.G. Sarantites [a], R.J. Charity [a], L.G. Sobotka [a], D.W. Stracener [a], D.C. Hensley [b], J.R. Beene [b], C. Baktash [b], M.L. Halbert, and [b] M. Thoennessen [b]

[a] *Oak Ridge National Laboratory Oak Ridge, Tennessee 37831, USA*

[b] *Department of Chemistry, Washington University, St. Louis, Missouri 63130, USA*

Abstract

The population of evaporation residue entry states in the decay of the compound nucleus $^{160}Er^*(54$ MeV) is investigated in a cross-bombardment employing the reactions $^{16}O + ^{144}Nd$ and $^{64}Ni + ^{96}Zr$. Evaporation residue cross sections and entry state γ-ray fold distributions of the dominant exit channels were obtained for each reaction, using a 4π γ-ray detection system. An entrance-channel dependence of the γ-ray fold distributions of the xn products is observed. This effect is described successfully by the statistical model making use of compound nucleus angular momentum distributions obtained with a fusion model that provides a good description of the bombarding energy dependence of fusion data for both reactions. In accordance with recent findings on the decay of $^{164}Yb^*$, it is suggested that the observed differences in the population of the dominant exit channels originate from the primary spin distributions rather than a possible dependence of the compound nucleus decay on the formation mode.

1 Introduction

The formation and decay of compound nuclei has always been of considerable interest in the study of heavy-ion reactions. In the near and below Coulomb barrier energy regime, the fusion cross sections (σ_{fus}) of many reaction systems has long been known to exhibit an enhancement over the predictions of one-dimensional barrier penetration models [1]. The advent of multidetector γ-ray detection systems made possible measurements of the evaporation residue spin distributions. In a few cases, the difficult task of the compound nucleus angular momentum distribution (σ_ℓ) reconstruction has been undertaken. Such measurements have indicated a broadening of the σ_ℓ-distributions

accompanying the subbarrier fusion cross section enhancements. Simultaneous measurements of σ_{fus} and σ_ℓ provides valuable information on the fusion process and a stringent test of the fusion models [2, 3].

In the rare earth region, certain studies have addressed the role of entrance-channel mass asymmetry on the population of the compound nucleus angular momentum [4-11]. For example, in the work of Haas et al. [5] the compound nucleus ^{160}Er* was produced via four reactions of considerably different mass asymmetries at common excitation energies. A dramatic entrance-channel dependence of the average evaporation residue γ-ray multiplicities was observed. The results were interpreted in terms of zero-point vibrations and the implied σ_ℓ-distributions were found sufficient to account for the evaporation residue yields and average γ-ray multiplicities calculated with the statistical model. The origin of these effects was also explained with simplified coupled-channel calculations [6]. Another interesting result has been reported by Ruckelshausen et al. [10] on the decay of ^{156}Er*(47 MeV) formed in the reactions ^{12}C + ^{144}Sm and ^{64}Ni + ^{92}Zr. Strong differences in the αxn and high spin xn populations were observed. Furthermore, a reconstruction of the (primary) σ_ℓ-distributions indicated an entrance-channel dependence of the ratio of the 2n/3n cross sections as a function of the compound nucleus spin. This suggested that there may be memory during the particle evaporation process, in contrast to the Bohr hypothesis concerning the independence of the compound nucleus decay on the formation mode.

Motivated by the previous results, Barreto et al. [11] studied the deexcitation of ^{164}Yb*(54 MeV) formed in the reactions ^{16}O + ^{148}Sm and ^{64}Ni + ^{100}Mo. Evaporation residue γ-ray fold distributions (k_γ) as well as energy and angular distributions of the emitted light charged particles were observed using 4π multidetector systems. A projectile breakup mechanism in the ^{16}O-induced reaction was found responsible for differences in the k_γ-distributions observed in the αxn products of these reactions. Furthermore, the γ-ray fold distributions of the xn products were found consistent with the predictions of the statistical model using σ_ℓ-distributions that describe closely measured fusion excitation functions for these systems. It was also pointed out that the shape of the σ_ℓ-distributions play a prominent role in the evaporation yields, especially for the mass-symmetric entrance channel [12].

In this paper, we present the results of a study [13] on the decay of ^{160}Er* produced in the reactions ^{16}O + ^{144}Nd and ^{64}Ni + ^{96}Zr at the excitation energy of $E^* \approx 54$ MeV. As in Ref. [11], the observed γ-ray fold distributions of the xn products show differences depending on the entrance channel. For the description of the fusion process in these systems, we make use of an one-dimensional barrier penetration model with energy-dependent barriers as applied in Ref. [12] for the reactions ^{16}O + ^{148}Sm and ^{64}Ni + ^{100}Mo. It is shown that the model accounts well for the measured energy dependence of

the average angular momentum in the $^{16}O + ^{144}Nd$ and $^{64}Ni + ^{96}Zr$ reactions [14, 15]. Employing the appropriate σ_ℓ-distributions in the statistical model results in a good description of all features of the $^{160}Er^*$ decay observed in the present work.

2 Experimental Procedures

Heavy-ion beams of ^{64}Ni (E_{lab} = 242.0 MeV) and ^{16}O (E_{lab} = 87.0 MeV), accelerated by the Oak Ridge HHIRF Tandem, bombarded highly enriched targets of ^{96}Zr and ^{144}Nd, respectively. The average beam energies where the reactions took place were estimated to be very close to the beam energies in the middle of the targets: $\sim$ 235.0 MeV and $\sim$ 85.6 MeV, respectively. The initial excitation energies of the compound nucleus $^{160}Er^*$ were estimated to be 54.5 MeV and 54.6 MeV in the ^{64}Ni and ^{16}O-induced reactions, respectively.

Light charged particles (p, d, ^3He, α)emitted in these reactions were detected by the Dwarf Ball; a nearly 4π CsI(Tl) scintillator array [16], consisting of 70 equal solid angle detectors covering laboratory angles from θ_{lab} = 12° to 168°. The energy calibration procedures were the same as in Ref. [11], where they are described in detail.

Residual nuclei were identified by their discrete γ-ray transitions, detected in an array of 18 Compton-suppressed Ge detectors inserted in the Oak Ridge Spin Spectrometer array [17]. The Ge array was always required to make an event trigger. Scaled-down events where the Ge detector was the trigger were stored in order to provide data for the (HI,xn) channels. The scale-down factor was adjusted in order to equalize approximately the rates of γ-particle coincidences and γ-ray singles stored during the data aquisition.

The γ-ray multiplicity distributions for each identified exit channel were measured using 52 NaI(Tℓ) detectors of the Spin Spectrometer and the 18 anti-Compton shields of the Ge detector array. For the NaI(Tℓ) detectors of the Spin Spectrometer good separation between neutron and γ-ray pulses was achieved by time-of-flight techniques, using the average "t_0" procedure described in Ref. [17]. For the anti-Compton shields, the limited timing resolution prevented the complete identification of neutron and γ-ray pulses. Energy and efficiency calibrations of the γ-ray detectors were obtained using γ-ray sources according to the procedures of Ref. [11]. The response functions of the Spin Spectrometer, providing the γ-ray multiplicity (M_γ) as a function of the γ-ray coincidence fold (k_γ), were obtained using data from the above sources in the equal energy approximation [17].

The experimental setup made possible the observation of the γ-ray fold dis-

tributions of channel-selected evaporation residues and the associated energy and angular distributions of the emitted charged particles. Absolute cross-sections were measured by integrating the beam current and correcting for the average effective charges, $\overline{q}_{Ni} = 21.47$ and $\overline{q}_O = 7.24$, determined for equilibrated projectile charge states in their passage through the target. The maximum systematic error in the cross-sections reported below is estimated to be $\simeq 17\%$.

Table 1 lists the measured evaporation residue cross-sections for the xn and αxn channels in the ^{64}Ni + ^{96}Zr and ^{16}O + ^{144}Nd reactions. These cross sections were obtained from the discrete γ-ray transitions given in the Table.

Table 1
Identifying transitions and experimental cross sections of evaporation residues observed in the present work.

Residue	Channel	E_γ (keV)	Transition	$\Delta k^a{}_\gamma$	$\sigma \pm \delta\sigma^b$ (mb)	$\sigma \pm \delta\sigma^b$ (mb)
					^{16}O + ^{144}Nd	^{64}Ni + ^{96}Zr
^{158}Er	2n	192.1	$2^+ \rightarrow 0^+$		6 ± 3	13 ± 3
^{157}Er	3n	266.4	$\frac{17}{2}^+ \rightarrow \frac{13}{2}^+$	2.75	165 ± 17	105 ± 10
^{156}Er	4n	344.6	$2^+ \rightarrow 0^+$		523 ± 50	113 ± 12
^{155}Er	5n	475.7	$\frac{17}{2}^+ \rightarrow \frac{13}{2}^+$	2.75	56 ± 6	$4.0^{+2.0}_{-4.0}$
^{154}Dy	α2n	334.5	$2^+ \rightarrow 0^+$		17 ± 2	4.9 ± 1.5
Total					767 ± 73	239 ± 16

a) Shift applied in the corresponding fold distributions.
b) Statistical error.

The measured angular and energy distributions of emitted protons and α-particles were transformed event-by-event in the center-of-mass (C.M.) system assuming two-body kinematics. In both systems, the αxn cross sections were found to be small. For ^{64}Ni + ^{96}Zr, the angular distributions of the α-particles associated with the αxn channels were found to be symmetric about 90° in the C.M. system. However, for ^{16}O + ^{144}Nd the angular distributions showed an excess of forward emitted α-particles in the α2n channel, a finding similar to the one observed in the previously studied ^{16}O + ^{148}Sm reaction [11]. A detailed analysis identified the origin of this component with an incomplete fusion process in which the ^{16}O projectile breaks up into ^{12}C + α, followed by fusion of ^{12}C with the target nucleus [11]. In the present work, we limit our discussion to the observables related to the most prominent xn decay channels.

Entry state distributions (in γ-ray fold and total γ-ray pulse height) of evap-

oration residues were extracted using the information provided by the Spin Spectrometer. The experimental k_γ-distributions of the odd mass evaporation residues were shifted by Δk_γ in cases where the gating γ-transition leads to a state of non-zero spin. The applied shifts are given in Table 1. This correction accounts for the number of γ-rays that would have been emitted if the ground state of the residual nucleus was zero or for those low-energy transitions which are below the energy threshold of the Spin Spectrometer (eg. ^{157,155}Er). It was assumed that $\Delta I = 2\Delta M_\gamma \approx 2\Delta k_\gamma$. This way, a direct comparison can be made between the experimental fold distributions and the calculated ones with the statistical model in which details of nuclear structure are ignored.

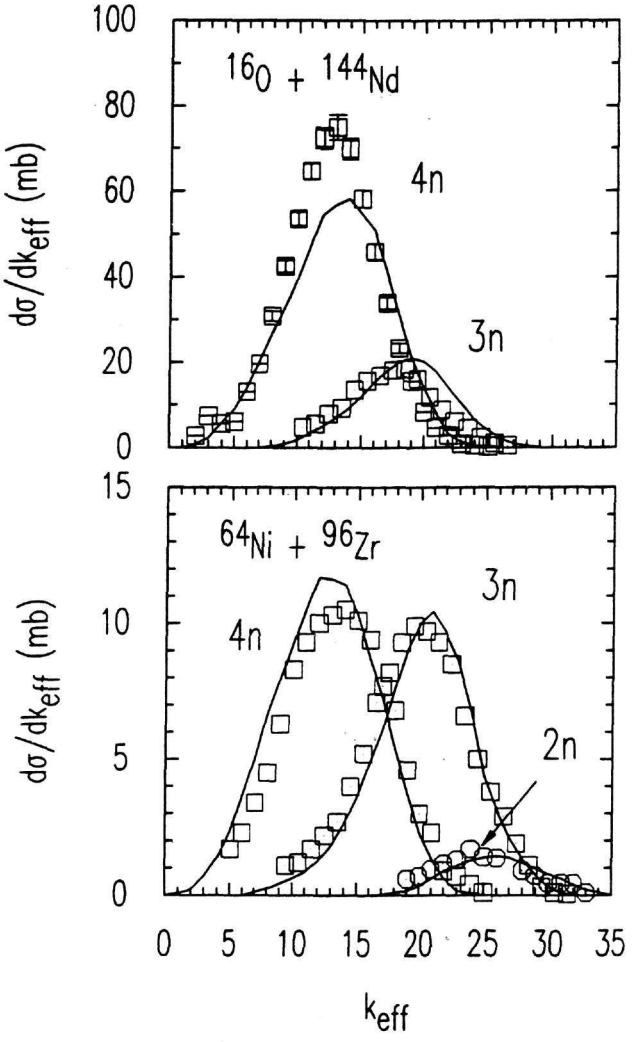

Fig.1. (a) Experimental γ-ray fold distributions of the observed xn channels in 87 MeV ^{16}O + ^{144}Nd reactions (symbols). The solid curves show the result of statistical model calculation described in the text. (b) Same as in (a), for 242 MeV ^{64}Ni + ^{96}Zr reactions.

Figure 1 shows the experimental γ-ray fold distributions of various xn channels as a function of $k_{eff} = k_\gamma + \Delta k_\gamma$, for the two reactions. Apart from the difference in the absolute magnitude of the respective cross sections, we observe the following features of the distributions for 4n and 3n channels: The k_γ-distributions in ^{64}Ni + ^{96}Zr are broader than in ^{16}O + ^{144}Nd. Furthermore, the centroids in ^{64}Ni + ^{96}Zr are displaced to a k_{eff}-value higher than in ^{16}O + ^{144}Nd. More specifically, the centroid of the 3n channel shows a displacement from k_{eff} = 20.0 to 17.6 and the 4n channel a smaller displacement from 12.5 to 13.6. Due to low statistics, the k_γ-distribution associated with the 2n channel in the ^{16}O + ^{144}Nd reaction is not shown.

It is of interest to investigate to what extent the above differences could indicate a possible dependence of the ^{160}Er* decay on the formation mode. However, the independence of formation and decay of the compound nucleus has to be examined in terms of the compound nucleus spin. Such an investigation requires knowledge of the relation between the evaporation residue γ-ray fold distributions and the (primary) compound nucleus spin distribution. This correspondence is obtained via the statistical model. Two approaches have previously been used for the comparison of the two reactions. In a first approach, one may attempt to deduce the compound nucleus spin distribution from the residue k_γ-distributions. This procedure was followed in Ref. [10] using techniques similar to those developed in Refs. [18-20]. This involves retrieving the compound nucleus angular momentum distribution by transforming from k_γ to γ-ray multiplicity (M_γ), then to the entry state spin, and finally to the compound nucleus spin. However, it has to be noted that the techniques of Refs. [18-20] are best suited for the transformation of distribution *averages* and not for *distributions*. More recently, a more refined event-by-event unfolding method was reported in Ref. [21].

To avoid problems with consecutive unfoldings, which may not give unique solutions in the case of tails of distributions, we have opted for the following approach [11]. Through the use of a fusion model we produce compound nucleus spin distributions (σ_ℓ) with parameters adjusted to fit measured fusion excitation functions for both reactions [14, 15]. In the subsequent statistical model calculations, the entry-state (E*,I), and the (E*,M_γ) distributions of each residue are obtained. By folding the (E*,M_γ) distributions with the measured (E*,M_γ) $\rightarrow$ (H_γ,k_γ) responses of the Spin Spectrometer, we obtain by projection the theoretical k_γ distributions which can be compared directly with the experimental ones.

3 Model Calculations

3.1 The Fusion Process

The measured total evaporation residue cross sections were found consistent with similar measurements of σ_{fus} and average angular momentum $\langle \ell \rangle$ performed by other groups on both reactions [14, 15].

In order to obtain realistic compound nucleus spin distributions under the bombarding energy conditions of the present experiment, we performed a model description of these data [13]. It was found that the one-dimensional barrier penetration model with a standard nuclear potential [22] was able to describe the above-barrier but underestimate the below barrier σ_{fus} and $\langle \ell \rangle$ data. This is a well known inadequacy of the one-dimensional barrier penetration model fordescribing the fusion of massive reaction systems at low subbarrier bombarding energies [1, 2].

It was realized that among the available fusion models, a simultaneous description of σ_{fus} and $< \ell >$ data may be provided by a recently introduced energy-dependent barrier penetration model [23]. This procedure makes use of the expression for the fusion cross section

$$\sigma_{fus}(E) = \frac{\pi}{k^2} \int (2\ell + 1) T_\ell(E) d\ell \tag{1}$$

where k is the asymptotic wavelength in the entrance channel and

$$T_\ell(E) = T_0[E - \frac{\ell(\ell+1)\hbar^2}{2\mu R^2}] \tag{2}$$

is the transmission coefficient for fusion. In Eq. 2, it is assumed that the barrier increases with ℓ by the addition of the centrifugal term $\ell(\ell+1)\hbar^2/2\mu R^2$. One obtains

$$\sigma_{fus}(E) = \frac{\pi R^2}{E} \int T_0(E') dE' \tag{3}$$

Therefore

$$\frac{d}{dE} \left| \frac{E\sigma}{\pi R^2} \right| = T_0(E) \tag{4}$$

Using the parabolic approximation of the fusion barrier,

$$T_0(E) = \{1 + exp[2\pi(B_{eff} - E)/\hbar\omega]\}^{-1} \tag{5}$$

whence

$$B_{eff} = E + (\hbar\omega/2\pi)ln[1 - T_0(E)]/T_0(E) \quad (6)$$

Once R and $\hbar\omega$ are specified, the effective barrier height B_{eff} can be determined from the experimental data. In the analysis of Ref. [23], R was treated as energy-independent and equal to the fusion barrier radius R_b implied by the near barrier data. The barrier curvature $\hbar\omega$ was determined from the extreme subbarrier data. It was shown that the extracted barriers exhibit the energy dependence suggested by the macroscopic model. A systematic analysis of fusion excitation functions [24] was also found consistent with these observations.

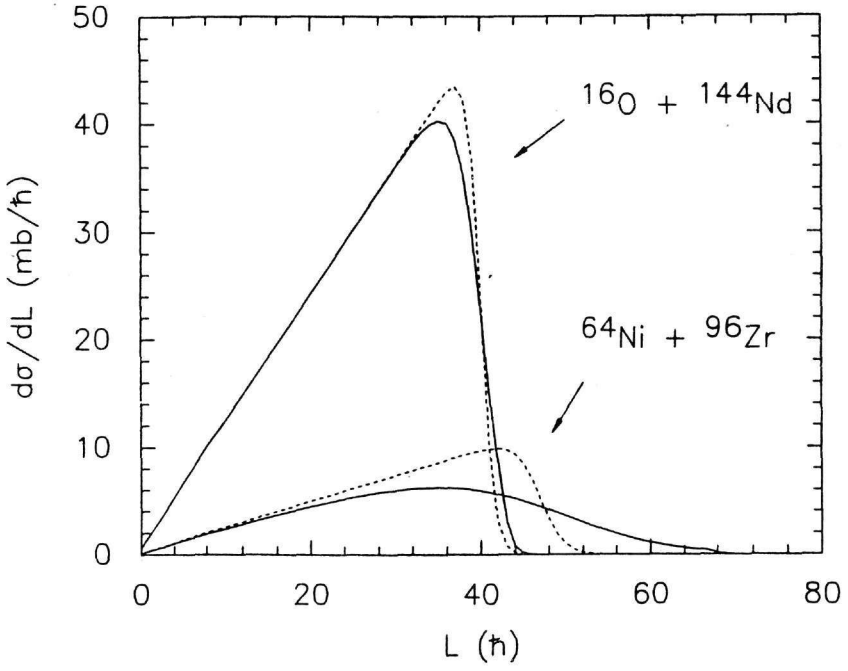

Fig.2. Spin distribution for E_{CM}=77 MeV $^{16}O + ^{144}Nd$ and E_{CM} = 141 MeV $^{64}Ni + ^{96}Zr$ according to the one-dimensional (dashed curve) and the energy-dependent barrier penetration model (solid curve).

For the purpose of creating spin distributions for the systems of the present study, we adopted the procedure of Refs. [23-25]. An energy-dependent fusion barrier

$$V_b(\epsilon) = \begin{cases} V_2, & \text{for } \epsilon > E_2 \\ V_1 + \frac{V_2 - V_1}{E_2 - E_1}(\epsilon - E_1) & \text{for } E_1 < \epsilon < E_2 \\ V_1, & \text{for } \epsilon < E_1 \end{cases}$$

was introduced in the one-dimensional barrier penetration model [12]. In our

calculations, the angular momentum dependence of the fusion barrier radii R_b and barrier curvatures $\hbar\omega$ was taken into account with nuclear potential parameters that describe closely the near-barrier data. V_1, V_2, E_1 and E_2 were treated as free parameters to fit the fusion excitation functions in an iterative procedure. This procedure resulted in an excellent fit of both the σ_{fus} and the $< \ell >$ excitation function data for both reactions [13]. Figure 2 shows the calculated primary spin distributions for both reactions under the bombarding energy conditions of the present study. Notice the differences between the distributions implied by the standard one-dimensional and the energy-dependent barrier penetration model.

3.2 The Compound Nucleus Decay

The decay of ^{160}Er* produced in the two reactions was described with the statistical model making use of the spin distributions produced with the energy-dependent barrier penetration model. The statistical model calculations were carried out with the code EVAP [26], using parameters typical of compound nuclei in the rare earth region.

For ^{16}O + ^{144}Nd, evaporation calculations were performed at the beam energy corresponding to the one in the middle of the target. This is justified by the fact that the fusion cross section in the energy region of interest is not steeply rising. By folding the calculated (E^*,M_γ) distributions with the measured (E^*,M_γ) $\rightarrow$ (H_γ,k_γ) responses of the Spin Spectrometer, we obtain by projection the theoretical k_γ distributions to be compared with the data. The comparison of the experimental and calculated distributions for the 3n and 4n channels is made in Fig. 1. The overall agreement is reasonably good despite a tendency of the calculation to overestimate the peak position of the distributions. This can be explained by the fact that the calculated fusion excitation function according to the data of [14] overestimates the measured cross section at the energy of the present study (Fig. 3 of Ref [13]), thus allowing for an excess of high-ℓ partial waves.

For ^{64}Ni + ^{96}Zr, detailed statistical model calculations were performed in order to take into account the energy loss of the beam through the target in connection with the steepness of the fusion excitation function (Fig. 4(a) of Ref. [13]). The target was divided into a number of slices, each representing an 1 MeV energy drop of the beam in the laboratory system. Statistical model calculations were performed at the beam energy in the middle of each slice. In each case, the k_γ-distributions of the xn products were deduced. The results of these calculations were averaged and compared with the experimental data. In Fig. 1 we show the comparison between the experimental and calculated k_γ-distributions of the 2n, 3n and 4n channels in the ^{64}Ni + ^{96}Zr reaction. The

overall agreement is good.

4 Discussion

In summary, we have observed apparent entrance channel effects in the spin distributions in evaporation residue cross sections in the reactions $^{16}O + ^{144}Nd$ and $^{64}Ni + ^{96}Zr$ producing $^{160}Er^*$ at the same excitation energy, that are similar to previous observations. The difference between the present work and earlier similar studies, e.g. Ref. [10], is that when realistic fusion models are used in the calculation of the input σ_ℓ distributions, then statistical model simulations that incorporate the detector responses reproduce satisfactorily the data. We find no need to resort to strong structural influences on the de-excitation of the compound nucleus. As in the work of Barreto *et al.* [11] the αxn channels are influenced by incomplete fusion processes that explain the observed differences. Finally, we point out that entrance channel effects in the early fusion dynamics [27] are important here. This is because reactions with different mass asymmetry can lead to differences in the early stages of the decay process. Sensitive probes, such as the $\gamma-$ray emission in the giant resonance region, are needed in this case to observe the differences [28]. In would be of great interest to find additional probes for these early dynamics effects.

Acknowledgements

J.L.B. acknowledges travel support from CNPq - Brazil, and Lafex-CBPF for use of its computer facilities for part of this work. This work was supported by the Director, Office of Energy Research, Office of High Energy and Nuclear Physics, Nuclear Physics Division of the US Department of Energy, under grant Nos. DE-FG02-88-ER40406 and DE-FG02-87-ER40316. Oak Ridge National Laboratory is managed by Martin Marietta Energy System, Inc. under Contract No. DE-AC05-84OR21400 with the Department of Energy.

References

[1] M. Beckerman, Rep. Prog. Phys. **51**, 1047 (1988).

[2] R. Vandenbosch, Annu. Rev. Nucl. Part. Sci. **42**, 447 (1992).

[3] D. E. DiGregorio and R. G. Stokstad, Phys. Rev. C **43**, 265 (1991).

[4] A. Charlop *et al.*, Phys. Rev. **C49**, R1235 (1994).

[5] B. Haas *et al.*, Phys. Rev. Lett. **54**, 398 (1985).

[6] C.H. Dasso and S. Landowne, Phys. Rev. C **32**, 1094 (1985).

[7] W. Kühn *et al.*, Phys. Rev. Lett. **62**, 1103 (1989).

[8] W. Kühn *et al.*, Phys. Rev. Lett. **51**, 1858(1983).

[9] D.J. Love *et al.*, Phys. Rev. Lett. **57**, 551 (1986).

[10] A. Ruckelshausen *et al.*, Phys. Rev. Lett. **56**, 2356 (1986).

[11] J.L. Barreto *et al.*, Phys. Rev. C **48**, 2881 (1993).

[12] N.G. Nicolis and D.G. Sarantites, Phys. Rev. C **48**, 2895 (1993).

[13] J.L. Baretto *et al.*, Phys. Rev. C**51**, 2584(1995).

[14] G. Duchène *et al.*, Phys. Rev. C **47**, 2043 (1993).

[15] A.M. Stefanini *et al.*, Nucl. Phys. A**548**, 453 (1992).

[16] D.W. Stracener *et al.*, Nucl. Inst. Meth. **A294**, 485(1990).

[17] M. Jääskeläinen *et al.*, Nucl. Inst. Meth. **204**, 385(1983).

[18] D.G. Sarantites *et al.*, Phys. Rev. C **18**, 774(1978).

[19] L. Westerberg *et al.*, Phys. Rev. C **18**, 796(1978).

[20] R.A. Dayras *et al.*, Phys. Rev. Lett. **42**, 697(1979).

[21] M. L. Halbert and J. R. Beene, in *Proceedings of the XIV Symposium on Nuclear Physics,* Cuernavaca, Mexico, January 7-10, 1991, ed. M.E. Brandan, World Scientific Publishers, 1991.

[22] Ö. Akyüz and A. Winther, in *Proceedings of the Enrico Fermi International School of Physics*, 1979, edited by R.A. Broglia, C.H. Dasso, and R. Ricci (North-Holland, Amsterdam, 1981), p. 492.

[23] V. S. Ramamurthy *et al.*, Phys. Rev. C **41**, 2702 (1990).

[24] A. K. Mohanty *et al.*, Phys. Rev. C**46**, 2012 (1992).

[25] A. K. Mohanty *et al.*, Phys. Rev. Lett. **65**, 1096 (1990).

[26] N. G. Nicolis, D. G. Sarantites and J. R. Beene. Computer code EVAP (unpublished); evolved from the code PACE by A. Gavron, Phys. Rev. C**21**, 230(1980).

[27] H. Feldmeier, Rep. Prog. Phys. **50**, 915 (1987).

[28] M. Thoennessen *et al.*, Phys. Rev. Lett. **70**, 4055(1993).